Coupled Systems Mechanics, *Vol. 15, No. 1 (2026) 47-60*
https://doi.org/10.12989/csm.2026.15.1.047

Techno-Press

A new improved solution to reduce the shear stress interface of a steel beam strengthened with composite materials

Hassaine Daouadji Maya[1,2], Hassaine Daouadji Tahar*[1,2], Bensatallah Tayeb[1,2]

[1]*Civil Engineering Department, University of Tiaret, Algeria*
[2]*Laboratory of Geomatics and sustainable development, University of Tiaret, Algeria*

(Received November 25, 2025, Revised January 8, 2026, Accepted February 6, 2026)

Abstract. This paper presents a novel approach to mitigate shear interface stress in steel beams reinforced with composite materials. The proposed solution is distinctive as it integrates shear strains from both the beam and the reinforcing plate, leading to improved accuracy in predicting critical interface stresses and the composite structure's overall behavior. The analysis is based on a parabolic shear stress distribution assumption across the thickness of both the steel beam and the bonded plate. A parametric analysis is conducted to explore various factors impacting the stability of the composite plate, acknowledging that interface stresses depend on the material and geometric properties of the reinforcement. The results show that parameter variations have a significant effect on maximum shear stresses within the composite material. Numerical findings substantiate the new solution's efficacy and elucidate key aspects of interfacial stress distributions. This research deepens the comprehension of mechanical interactions at the interface and supports the design process for composite-steel hybrid structures.

Keywords: interfacial stresses; prestressed composite plate; shear lag effect; steel beam; strengthening

1. Introduction

This paper aims to study the mechanical behavior of steel beams reinforced with externally bonded composite materials, a promising solution for rehabilitating existing structures to counter natural phenomena like earthquakes and changes in building use. Composites are a promising solution to avoiding demolition and new construction, but the most important failure mode is the detachment of the composite material plate due to high interface stresses near the edge of the bonded plate [1-3]. An improved method for calculating interface stresses was developed in this study [4-13]. Interfacial stress studies have been conducted to predict adhesive-adherend interface shear stresses, but accounting for the influence of adherend shear deformation is rare [14-21]. Shear stresses are developed in the adhesive zone and they are continuous across the interface which equilibrium requires zero stress at the free surface. Tounsi [1] extended this theory to study concrete beams strengthened by composite plates. The basic assumption in these studies is a linear distribution of shear stress across the thickness of the adherends. However, beam theory assumes a parabolic distribution through the depth of the beam. To address this, a solution methodology should be developed that better accounts for the effect of adherend shear deformations. This paper

*Corresponding author, Professor, E-mail: daouadjitahar@gmail.com

ISSN: 2234-2184 (Print), 2234-2192 (Online)

aims to present an improvement of the solution to obtain a new closed-form solution that accounts for the parabolic shear deformation effect in both the beam and bonded plate, and compare it quantitatively with the new one developed in this paper [22-33].

The study focuses on the maintenance and upkeep of civil engineering structures, specifically the detachment of the reinforcing plate. The authors analyze the anisotropic nature of composite materials and assume a parabolic distribution of stresses through the adhesive layer. They find that the maximum interface stresses calculated by this method align perfectly with literature. Recent techniques, such as carbon fiber composite bonding, have shown promising results. The paper aims to demonstrate how the mechanical and geometric characteristics of composite materials can reduce the influence of interface stresses, ensuring the stability of reinforced metal beams. Four innovative solutions are proposed to maintain the composite plate bonded to the steel beam, based on plate characteristics and applied forces. The proposed solutions aim to reduce shear stresses at the end of a composite material plate. Key methods for structural rehabilitation include extending reinforcement strips to supports, applying prestressing forces, using thin composite plates, and optimizing the geometry of composite material plate ends bonded to steel beams. These solutions are expected to improve practical design for structural reliability and increase the fatigue life of structures. The manuscript will discuss these solutions.

2. Mathematical formulation of the proposal

2.1 Research significance

The debonding of composite material plates in composite-strengthened steel beams is a prevalent failure mode that hinders the beams from achieving their maximum flexural capacity, mainly due to shear stress concentrations in the adhesive layer. To establish design guidelines for strengthening these beams, solutions for stress concentrations are necessary. A new solution proposed considers three parameters related to reinforcement methods to minimize shear interface stress. The study examines the effects of the reinforced region on plate length, the role of composite plate prestressing on adhesive stress, and the optimization of edge geometry to reduce interfacial shear stress. Additionally, an economical dimensioning method is proposed that incorporates the parabolic shear deformation effect in bonded plates, offering a comparison with previous solutions.

2.2 Basic assumptions

This study examines the structural model and steps involved in strengthening a beam with a bonded prestressed laminate (Figs. 1 and 2). It considers transverse shear stress and strain in the beam and plate, but ignores transverse normal stress. The analysis uses Hassaine Daouadji's [30] analytical approach for steel beam strengthened with a bonded prestressed composite plate to compare it with other analytical solutions. The study also includes an infinitesimal element of the reinforced steel beam.

The analytical approach is based on the following assumptions [30]:

- Bending deformations of the adhesive are neglected, the adhesive is assumed to only play a role in transferring the stresses from the steel beam to the prestressed carbodur composite plate reinforcement.

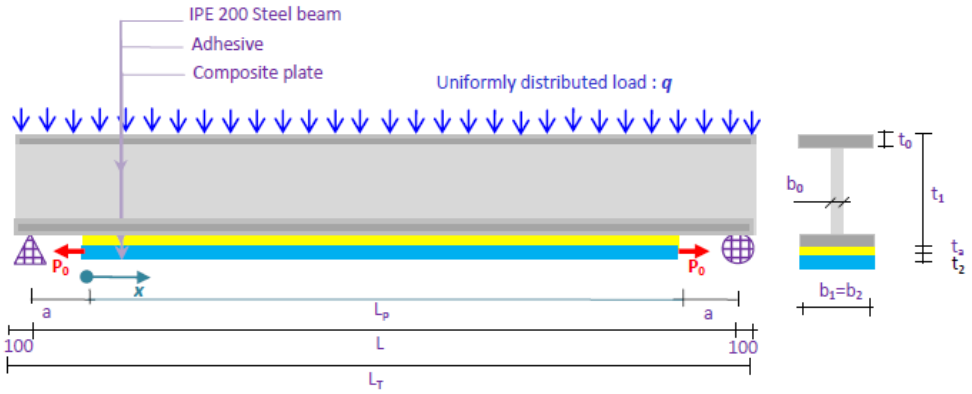

Figure 1. Steel beam bonded by a prestressed composite plate

- No slip is allowed at the interface of the bond, there is a perfect bond between the prestressed carbodur composite plate and the steel beam.
- All materials considered are linear elastic for steel beam, prestressed carbodur composite plate and adhesive.
- The steel beam is simply supported and shallow, i.e., plane sections remain plane in bending.
- The stresses in the adhesive layer do not change through the direction of the thickness.
- The shear stress analysis presumes equal curvatures in the beam and plate, differing from the peel stress approach. As the beam is loaded, vertical separation occurs between the steel beam and the carbodur composite plate, as noted in studies by Tounsi [1] and Smith and Teng [3].
- A parabolic shear stress distribution through the depth of both the steel beam and the bonded carbodur composite plate is assumed.

2.3 Shear stress distribution along the composite-steel beam interface

The theory can be expressed by cutting out a differential section *dx* from a composite-strengthened steel beam, illustrating the strains near the adhesive interface and the external composite plate reinforcement, as shown in Fig. 2.

The deformation in Steel beam in the vicinity of the adhesive layer can be expressed by Hassaine Daouadji [30]:

$$\varepsilon_1(x)=\frac{du_1(x)}{dx}=\frac{y_1}{E_1I_1}M_1(x)+\frac{N_1(x)}{E_1A_1}+\frac{t_1}{4G_1}\frac{d\tau(x)}{dx} \tag{1}$$

Based on the theory of laminated sheets, the deformation of the composite sheet in the vicinity of the adhesive layer is given by:

$$\varepsilon_2(x)=\frac{du_2(x)}{dx}=-\frac{y_2}{E_2I_2}M_2(x)+\frac{P_0+N_2(x)}{E_2A_2}+\frac{5t_2}{12G_2}\frac{d\tau(x)}{dx} \tag{2}$$

Where $u_1(x)$ and $u_2(x)$ are the horizontal displacements of the Steel beam and the composite plate respectively. $M_1(x)$ and $M_2(x)$ are respectively the bending moments applied to the Steel beam and the composite plate; P_0 is the compression force in the beam due to prestressing, E_1 is the Young's modulus of steel; I_1 the moment of inertia the steel beam, E_2 is the Young's modulus of

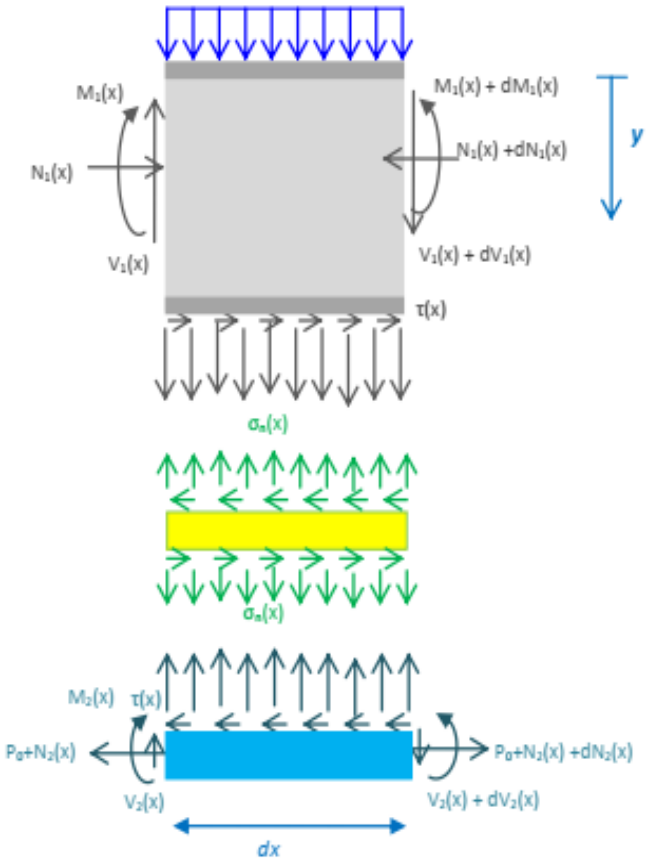

Figure 2. Forces in infinitesimal element of a steel beam bonded by composite plate

the composite plate; I_2 the moment of inertia the composite plate, N_1 and N_2 are the axial forces applied to the Steel and the composite plate respectively, b_2 and t_2 are the width and thickness of the reinforcement plate.

The reinforcement plate's stiffness is significantly lower than the steel beam to be reinforced, and the bending moment in the composite plate can be neglected for simplified shear stress derivation operations. The shear stress at the adhesive layer can be expressed as follows:

$$\tau_a = \tau(x) = K_s \Delta u(x) = K_s \left[u_2(x) - u_1(x)\right] \tag{3}$$

Where K_s is the shear stiffness of the adhesive layer per unit length. From equation (3) we can deduce the expression of K_s which is given by:

$$K_s = \frac{\tau(x)}{\Delta u(x)} = \frac{\tau(x)}{\Delta u(x)/t_a}\frac{1}{t_a} = \frac{G_a}{t_a} \tag{4}$$

$\Delta u(x)$ is the displacement relative to the adhesive interface, G_a and t_a are the shear modulus and thickness of the adhesive layer, respectively. By differentiating the Eqs. (3), (1) and (2) with respect to x, and neglecting the bending moment of the composite plate and by differentiating the resulting equation, we will have:

$$\frac{d^2\tau(x)}{dx^2} = K_s\left[\left(\frac{1}{E_2A_2}\frac{dN_2(x)}{dx} - \frac{y_2}{E_2I_2}\frac{dM_2(x)}{dx}\right) - \left(\frac{y_1}{E_1I_1}\frac{dM_1(x)}{dx} + \frac{1}{E_1A_1}\frac{dN_1(x)}{dx}\right)\right] - K_s\left(\frac{5t_2}{12G_2} + \frac{t_1}{4G_1}\right)\frac{d^2\tau(x)}{dx^2} \quad (5)$$

Substituting $dM_1(x)/dx$, $dM_2(x)/dx$ and $N(x)$ with their following expressions in Eq. (5):

$$N_1(x) = -N(x) = -N_2(x) = -b_2\int_0^x \tau(x) \quad (6)$$

$$\frac{dM_1(x)}{dx} = \frac{E_1I_1}{E_1I_1 + E_2I_2}\left[V(x) - b_2\tau(x)\left(y_1 + t_a + \frac{t_2}{2}\right)\right] \quad (7)$$

$$\frac{dM_2(x)}{dx} = \frac{E_2I_2}{E_1I_1 + E_2I_2}\left[V(x) - b_2\tau(x)\left(y_1 + t_a + \frac{t_2}{2}\right)\right] \quad (8)$$

Allows us to obtain the differential equation of the shear interface stress:

$$\frac{d^2\tau(x)}{dx^2} - \frac{b_2\left[\frac{(y_1+y_2)(y_1+y_2+t_a)}{E_1I_1+E_2I_2} + \frac{1}{E_1A_1} + \frac{1}{E_2A_2}\right]}{\frac{t_a}{G_a} + \frac{t_1}{4G_1} + \frac{5t_2}{12G_2}}\tau(x) + \frac{\left[\frac{y_1+y_2}{E_1I_1+E_2I_2}\right]}{\frac{t_a}{G_a} + \frac{t_1}{4G_1} + \frac{5t_2}{12G_2}}V(x) = 0 \quad (9)$$

The general solution provided is applicable solely to concentrated loads or uniformly distributed loads, such as those observed in the case study, affecting a specific section of the reinforced beam. For such loading, $d^2V(x)/dx^2=0$, and the general solution to Eq. (9) is given by

$$\tau(x) = \phi_1\cosh(\Delta x) + \phi_2\sinh(\Delta x) + \frac{(t_1+t_2)}{2\Delta^2\left(\frac{t_a}{G_a} + \frac{t_1}{4G_1} + \frac{5t_2}{12G_2}\right)(E_1I_1+E_2I_2)}V(x) \quad (610$$

Where:

$$\Delta = \left[\frac{b_2\left[\frac{(t_1+t_2)(t_1+t_2+2t_a)}{4(E_1I_1+E_2I_2)} + \frac{1}{E_1A_1} + \frac{1}{E_2A_2}\right]}{\frac{t_a}{G_a} + \frac{t_1}{4G_1} + \frac{5t_2}{12G_2}}\right]^{\frac{1}{2}} \quad (11)$$

And ϕ_1 and ϕ_2 are constant coefficients determined from the boundary conditions. The study examines a beam that is simply supported and subjected to a uniformly distributed load. The formula for shear stress in a uniformly distributed load is given by the following equation:

$$\tau(x) = \left[\Delta^{-1}\left(\frac{t_a}{G_a} + \frac{t_1}{4G_1} + \frac{5t_2}{12G_2}\right)\left(\frac{E_2}{b_2}P_0 - \frac{y_1M_t(0)}{E_1I_1}\right)\right]e^{-\Delta x} + \frac{(t_1+t_2)\left(a_1q_1 + x - \frac{e^{-\Delta x}}{\Delta}q_1\right)}{2\Delta^2\left(\frac{t_a}{G_a} + \frac{t_1}{4G_1} + \frac{5t_2}{12G_2}\right)(E_1I_1+E_2I_2)} \quad (12)$$

$$0 \le x \le L_P$$

3. Results and discussions

3.1 Material used

Table 1. Geometric and mechanical properties of the materials used

Component	Width (mm)	Depth (mm)	Young's modulus (MPa)	Poisson's ratio
Adhesive layer "Sikadur 30"	b_a=100	t_a=2	E_a=12 800	0.35
Sika Carbodur composite plate	b_2=100	t_2=1,2	E_2= 165 000	0.28
Steel beam IPE 200	b_1=100	t_1=200	E_1= 210 000	0.30

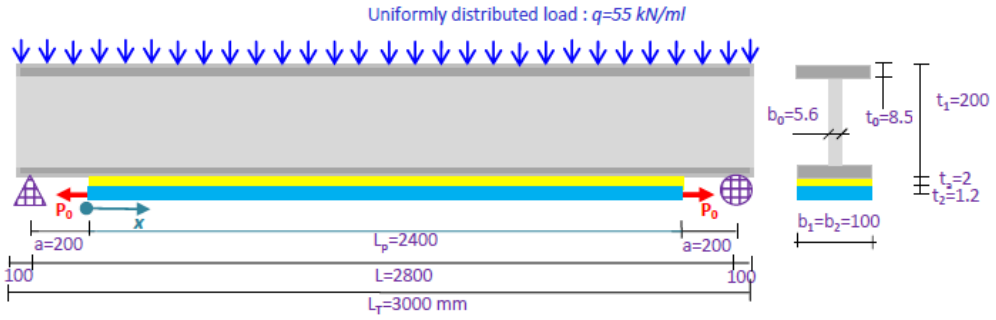

Figure 3. Geometric characteristic of a steel beam bonded by a prestressed composite plate

The study investigates the performance of a steel beam reinforced with a prestressed composite plate under uniformly distributed load conditions. Key materials and configurations critical to understanding the beam's behavior include steel for the beam, cabodur for the reinforcing plate, and sikadur 30 as the adhesive. These elements play a significant role in the structural integrity and load-bearing capacity of the beam. A summary of the geometric and material properties is given in Table 1 and Fig. 3. The span of the steel beam is L_p=2400 mm, the distance from the support to the end of the plate is a=200 mm and the uniformly distributed load is q=55 kN/ml.

3.2 Comparison with analytical solutions

The model is validated using a steel section IPE 200 and a steel beam reinforced with sika carbodur composite plate (Fig. 3). The beam is supported and subjected to three-point bending, and the predicted analytical results are in reasonable agreement with the experimental results of the Hassaine Daouadji study [30]. The use of composite materials with glues on stretched surfaces is an effective way to reinforce structural beams, especially for undersized beams (Fig. 4). Bonding of the composite on tensioned surfaces increases the ultimate strength of reinforced beams and decreases deflection, thereby improving the durability of reinforced structures.

The present solution is verified by comparing it with typical analytical solutions using Model Hassaine Daouadji [30]. This model ensures continuity in research and corrects the results obtained. For example, the strengthening of a steel beam is compared without and with considering prestressing force (P_0=0, P_0=10 kN and P_0=20 kN). The interface shear stress distributions obtained by the present study and other existing models are shown in good agreement. As demonstrated, good agreements of the interface shear stress among all the comparisons are reached at the plate end. In this section, numerical results of the present solution are presented to study the effect of the prestressing force P_0 on the distribution of interface shear stress in steel beam strengthened with bonded prestressed carbodur composite plate. We have registered the maximum shear stress occurring at the ends of adhesively bonded plates. In addition,

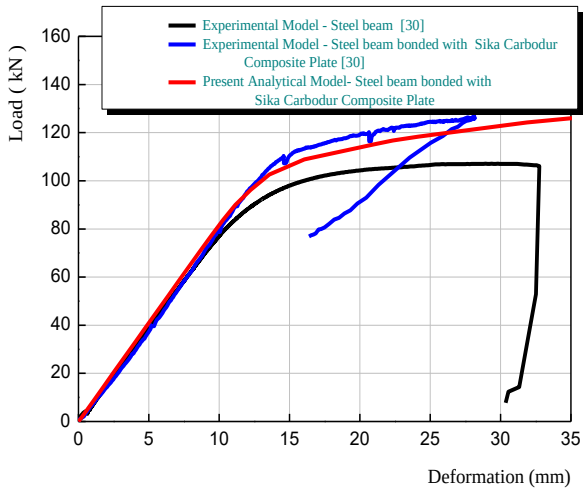

Figure 4. Comparison of the structural response between the analytical and experimental study for the steel beams reinforced with cardodur composite plate

Table 2. Comparison of interfacial shear stresses for steel beams reinforced with composite plates using the present approach with existing analytical solutions in the literature

Steel beam bonded by a prestressed composite plate under uniformly distributed load						
	Model Hassaine Daouadji [30]			Present model		
Prestressing load (kN)	P_0= 0	P_0= 10	P_0= 20	P_0= 0	P_0= 10	P_0= 20
Interfacial Shear stress (MPa)	5,9363	-1,9301	-9,7979	5,8678	-1,8809	-9,6297

we observe that an increase in the value of the prestressing force P_0 leads to a reduction in shear stress concentrations.

3.3 Composite plate-related parameters influencing the reduction of interfacial shear stresses

After verifying the accuracy of the present analytical model, a parameter study related to the geometry of the reinforcing composite plate influencing the reduction of interfacial shear stresses is carried out to better understand the effects of the proposed new solutions on the reduction of interfacial stresses under the coupling of different applied loads (q and P_0).

3.3.1 Effect on plate length of the strengthened steel beam region

Fig. 5 illustrates the relationship between the length of the ordinary beam region and edge shear stresses. It indicates that as the plate is positioned further from the supports, interfacial shear stresses notably diminish. Consequently, in scenarios of strengthening, particularly retrofitting in areas of peak bending moments at midspan, it is advisable to extend the strengthening strip closer to the supports. The findings demonstrate that lengthening the composite reinforcement plate to the supports nearly eliminates maximum shear stress, thereby enhancing the stability of the reinforced beam. This outcome supports the study's objectives by preventing detachment of the composite plate and maintaining the reinforced beam's structural integrity.

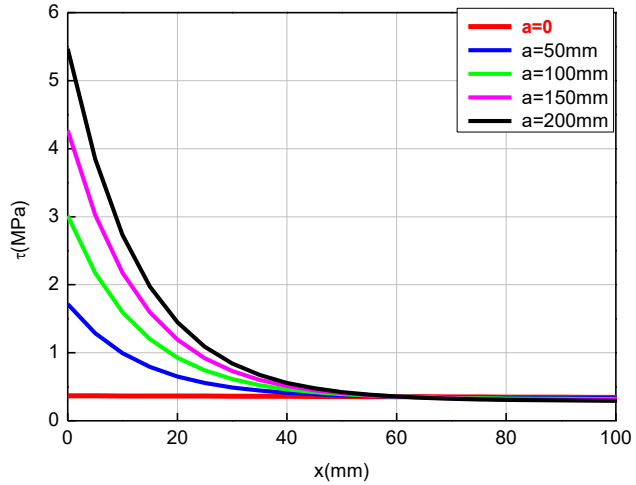

Figure 5. Effect on plate length of the strengthened steel beam region

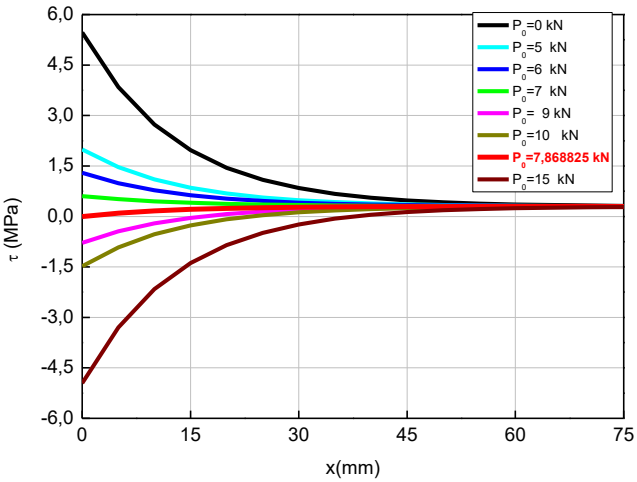

Figure 6. Effect of prestressing force (P_0) of composite plate on adhesive shear stress

First solution suggestion: The first solution aims to reduce shear stresses at the end of a composite plate by extending the reinforcement strip to the supports as much as possible. This is recommended to eliminate the concentration of shear stress at the edge, as previous research has shown that extending the reinforcement strip can solve this issue.

3.3.2 Effect of prestressing force (P_0) of composite plate on adhesive stress

This study examines the impact of prestressing force P_0 on the distribution of interfacial stress in a steel beam strengthened with prestressed carbodur composite plate. Seven values of P_0 (P_0=0; P_0=5 kN, P_0=6 kN, P_0=7 kN, P_0=9 kN, P_0=10 kN and P_0=15 kN) are considered, and Fig. 6 shows the interfacial shear stress plotted for uniformly distributed load for the steel beam strengthened with prestressed carbodur composite plate. The results provide insights into the behavior of the steel beam under uniform load distribution, from these results, one can observe:

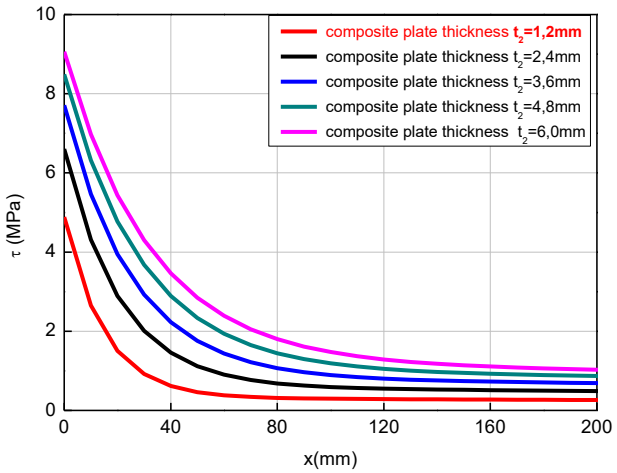

Figure 7. Effect of composite plate thickness

- The maximum shear stress occurs at the ends of adhesively bonded plates, which, upon peeling, disappears around 45 mm from the end and becomes very weak.
- The study reveals that increasing the prestressing force P_0 significantly decreases shear stress concentrations.
- The study applied a prestressing force of P_0=7.868825 kN, reducing the maximum shear stress to almost zero, ensuring the stability of the reinforced beam and preventing debonding of the composite plate, thus fulfilling the objective of the study.

Following the study and analysis of the prestressing force's effect, it was found that a prestressing value (P_0) of zero poses a risk of detachment for the reinforcement plate. However, when the prestressing value reaches approximately P_0=6 kN, a notable decrease in shear stress is observed, which indicates that the composite plate achieves stability and mitigates detachment risks. The critical value for eliminating shear interface stress is determined to be P_0 equal to 7.868825 kN. At this value, the stability of the composite plate is assured; otherwise, the composite remains adhered to the steel beam. Consequently, this condition leads to an increase in the stiffness of the hybrid steel-composite beam. The stability of the beam is maintained as long as the load remains below the critical threshold, which is 7.868825 kN. Exceeding this value will compromise the beam's structural integrity and stability.

Second solution proposal: The second solution reduces shear stress at the composite plate end, addressing the problem of debonding of the reinforcement plate. It is recommended to apply a prestressing force that cancels or reduces interface stresses before in situ bonding to steel beams.

3.3.3 Effect of composite plate thickness

The thickness of a composite plate plays a crucial role in determining the interfacial shear stresses and affects the bending resistance of hybrid steel-composite beams. This relationship is particularly significant as the rigidity of the hybrid beam increases. Fig. 7 shows that the thickness of the carbodide composite plate significantly influences these stresses. As the thickness increases, the interfacial shear stresses increase. Typically, composite plates used in practical engineering are smaller than steel plates, making the smaller interfacial shear stress level and concentration an advantage for retrofitting with composite plates compared to steel plates. The study found that a

thinner composite plate reduces shear stresses, ensuring the stability of the composition plate and preventing detachment. Therefore, a thin reinforcement plate can be used, resulting in maximum reduction in shear stress, ensuring the stability of the reinforced beam. This is the desired outcome for this study, ensuring stability and preventing detachment of the composite plate.

Third solution proposal: The third solution aims to reduce shear stress at the end of a composite plate, highlighting the importance of the thickness in design and addressing the problem of reinforcement plate detachment. Thin composite plates are recommended to reduce shear stress concentration at the edge, offering an economic advantage.

3.3.4 Geometric edge shape based optimization for interfacial shear stress reduction

The study identifies two intervals in the plate's variable end sections for geometric edge shape-based optimization for interfacial shear stress reduction, Since the end section of the plate is variable, we generally distinguish two intervals in which the thickness is, as indicated in the Eqs. (13a) and (13b):

$$t_2 = t(x) \quad \text{for} \quad 0 \le x \le a \tag{13a}$$

$$t_2 = \text{constant for} \quad a \le x \le \frac{l_p}{2} \tag{13b}$$

Applying the principle for the three cases: constant thickness (Fig. 8(a)), taper end section with linear variation (Fig. 8(b)), and stepped end section (Fig. 8(c)), the equations are written as follows:

- Constant thickness:

$$t_2(x) = t_2 \quad \text{for} \quad 0 \le x \le a \tag{14a}$$

$$t_2(x) = t_2 \quad \text{for} \quad a \le x \le \frac{l_p}{2} \tag{14b}$$

- Taper end section: linear variation:

$$t_2(x) = t_e + \frac{t_2 - t_e}{a} x \quad \text{for} \quad 0 \le x \le a \tag{15a}$$

$$t_2(x) = t_2 \quad \text{for} \quad a \le x \le \frac{l_p}{2} \tag{15b}$$

- Stepped end section:

$$t_2(x) = t_e \quad \text{for} \quad 0 \le x \le a \tag{16a}$$

$$t_2(x) = t_2 \quad \text{for} \quad a \le x \le \frac{l_p}{2} \tag{16b}$$

Case of taper end plate section (Fig. 8(b)): The study compares the geometric details of a composite plate with a taper end plate section to a uniform cross section (Fig. 8(a)) end plate. The results show (Fig. 9) that using a tapered end plate reduces interfacial shear stresses by about 40%, which is easy to achieve in situ when strengthening a steel beam in service. This reduction is

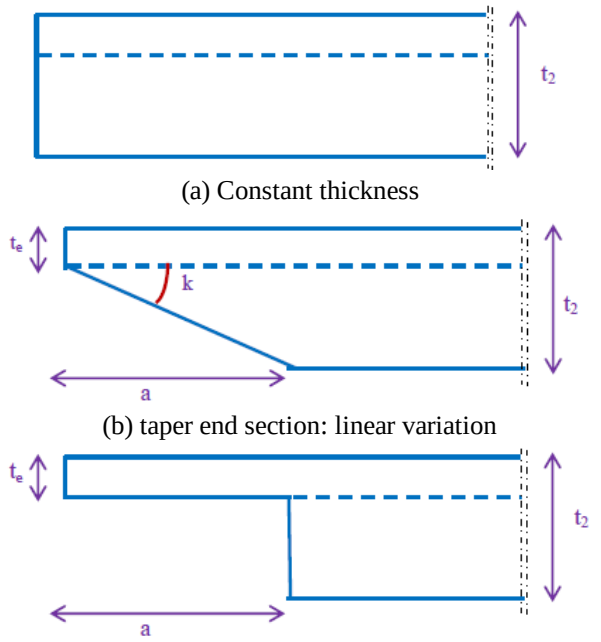

Figure 8. Geometric shape of end section of plate (a) constant thickness (b) taper end section: linear variation (c) stepped end section

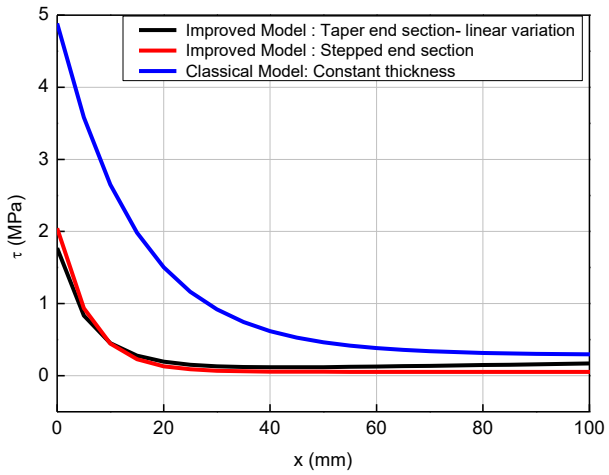

Figure 9. Effect of geometric edge shape-based optimization for interfacial shear stress reduction

significant from a design perspective.

Case of stepped end plate section (Fig. 8(c)): In this part another geometric configuration is analyzed. The end section of the composite plate has a stepped form as shown in Fig. 8(c). Here again, the results obtained by the analytical approach show a decrease in interfacial shear stresses compared to the uniform plate end cross section case. Fig. 9 shows the shear stress evolution caused by using stepped plate end section with respect to uniform plate end section. The results

obtained show that the shear stresses in this case are reduced by about 38% compared to the standard uniform cross section plate end.

Fourth solution proposal: Consequently, we present this fourth solution, which reduces shear stresses at the end of the composite plate. We have previously shown that varying the thickness of the composite plate is an important design in practice, as it can solve the problem of debonding of the reinforcement plate. We observed a gain of approximately 40%. It is recommended to use composite plates with a variable cross-section (thin at the ends) to reduce the concentration of shear stresses at the edges. This solution also offers a remarkable economic advantage.

4. Conclusions

This study investigates the interfacial stresses and bending behavior in steel beams that are reinforced with composite plates. It introduces a method to mitigate the edge effect during reinforcement by reducing shear stress at the ends of the composite plates. The findings suggest that optimal parameters improve bending performance by enhancing structural stiffness and reducing deformation. Solutions proposed to minimize interface shear stresses at the composite plate's end include: extending the composite plate to the supports to eliminate shear stress concentration, applying a prestressing force on the composite plate prior to bonding to the steel beam, utilizing thinner composite plates to address structural and economic concerns, and optimizing the geometric shape of the plate ends to achieve an approximate 40% gain in performance. Specifically, using variable sectional composite plates that are thinner at the ends can effectively reduce shear stress concentrations while also providing economic advantages.

The results obtained show an enhancement in practical design for structural reliability and a longer fatigue life of structures. While the present model is based on linear elasticity assumptions, it is suggested that future research incorporate material nonlinearities and complex stress distributions for better prediction accuracy. Such advancements would provide a more comprehensive understanding of structural behavior in realistic operating conditions.

References

1. Tounsi, A., Daouadji, T.H., Benyoucef, S. (2009). Interfacial stresses in FRP-plated RC beams: effect of adherend shear deformations. International Journal of Adhesion and Adhesives, 29(4), 343-351. https://doi.org/10.1016/j.ijadhadh.2008.06.008.
2. Daouadji, T.H. (2013). Analytical analysis of the interfacial stress in damaged reinforced concrete beams strengthened by bonded composite plates. Strength of Materials, 45(5), 587-597. https://doi.org/10.1007/s11223-013-9496-4.
3. Smith, S.T., Teng, J.G. (2001). Interfacial stresses in plated beams. Engineering Structures, 23(7), 857-871. http://doi.org/10.1016/S0141-0296(00)00090-0.
4. Ameur, M., Tounsi, A., Benyoucef, S., Bachir Bouiadjra, M., Adda Bedia, E.A. (2009). Stress analysis of steel beams strengthened with a bonded hygrothermal aged composite plate. International Journal of Mechanics and Materials in Design, 5(2), 143-156. https://doi.org/10.1007/s10999-008-9090-2.
5. Nguyen, D.D., Ta, H.D., Dao, D.S., Nguyen, H.D. (2025). Column buckling under stochastic three-dimensional material properties: a stochastic finite element analysis. Coupled Systems Mechanics, 14(4), 347-369. https://doi.org/10.12989/csm.2025.14.4.347.
6. Hung, C.C., Huandi, H., Nguyen, T., Hsieh, C.Y. (2025). Smart design of steel fiber effects on soft

computing of steel fiber reinforced self-compacting concrete. Coupled Systems Mechanics, 14(3), 247-267. https://doi.org/10.12989/csm.2025.14.3.247.
7. Daouadji, T.H. (2017). Analytical and numerical modeling of interfacial stresses in beams bonded with a thin plate. Advances in Computational Design, 2(1), 57-69. https://doi.org/10.12989/acd.2017.2.1.057.
8. Baghdadi, M., Bellali, M.A., Campilho, R.D., Serier, B. (2025). Optimization of composite patch designs for enhanced repair efficiency in damaged aircraft structures. Structural Engineering and Mechanics, 94(4), 299-311. https://doi.org/10.12989/sem.2025.94.4.299.
9. Benachour, A., Benyoucef, S., Tounsi, A. (2008). Interfacial stress analysis of steel beams reinforced with bonded prestressed FRP plate. Engineering Structures, 30(11), 3305-3315. https://doi.org/10.1016/j.engstruct.2008.05.007.
10. Wang, B., Yang, Z., Cai, W.Z., Shi, Q.X., Li, H., Yang, Y.L. (2025). Prediction and analysis of shear capacity for T-shaped RC squat walls. Structural Engineering and Mechanics, 93(3), 181. https://doi.org/10.12989/sem.2025.93.3.181.
11. Ripoll, L., Perez-Aparicio, J.L., Maimi, P., Gonzalez, E.V. (2023). Analytical crack growth in unidirectional composite flywheel. Coupled Systems Mechanics, 12(2), 183-197. https://doi.org/10.12989/csm.2023.12.2.183.
12. Hamrat, M., Bouziadi, F., Boulekbache, B., Daouadji, T.H., Chergui, S., Labed, A., Amziane, S. (2020). Experimental and numerical investigation on the deflection behavior of pre-cracked and repaired reinforced concrete beams with fiber-reinforced polymer. Construction and Building Materials, 249, 118745. https://doi.org/10.1016/j.conbuildmat.2020.118745.
13. Suarez-Suarez, A., Dominguez-Ramirez, N., Susarrey-Huerta, O. (2023). Numerical formulation solid-layer finite element to simulate reinforced concrete structures strengthened by over-coating. Coupled Systems Mechanics, 12(6), 481-501. https://doi.org/10.12989/csm.2023.12.6.481.
14. Saini, K., Lalthazuala, R., Singh, T.G. (2025). Flexural behaviour of hybrid high-strength steel I-beams. Steel and Composite Structures, 55(4), 319. https://doi.org/10.12989/scs.2025.55.4.319.
15. Daouadji, T.H., Rabahi, A., Abbes, B., Adim, B. (2016). Theoretical and finite element studies of interfacial stresses in reinforced concrete beams strengthened by externally FRP laminates plate. Journal of Adhesion Science and Technology, 30(12), 1253-1280. https://doi.org/10.1080/01694243.2016.1140703.
16. Mouffoki, A., Azab, M., Aicha, B., Belhocine, A., Aicha, R., Daikh, A.A., ... Tounsi, A. (2025). A novel integral parabolic plate theory incorporating stretching effects for the bending analysis of advanced FG plates resting on Winkler–Pasternak foundations. Coupled Systems Mechanics, 14(5), 451. https://doi.org/10.12989/csm.2025.14.5.451.
17. Kožar, I. (2024). Analysis of 3D pendulum sliding along a rope. Coupled Systems Mechanics, 13(5), 459-470. https://doi.org/10.12989/csm.2024.13.5.459.
18. Daouadji, T.H., Abbès, B., Bensatallah, T., Abbès, F. (2025). Analysis of interface sliding in a composite I-steel–concrete beam reinforced by a composite material plate: the effect of concrete–steel connection modes. Journal of Composites Science, 9(6), 273. https://doi.org/10.3390/jcs9060273.
19. Ljukovac, S., Ibrahimbegović, A., Cohodar-Husic, M. (2024). Time varying LQR-based optimal control of geometrically exact Reissner's beam model. Coupled Systems Mechanics, 13(1), 73. https://doi.org/10.12989/csm.2024.13.1.073.
20. Nguyen, P.T., Vi, T.V., Nguyen, T.T., Vu, V.T. (2023). The plate on the nonlinear dynamic foundation under moving load. Coupled Systems Mechanics, 12(1), 83-102. https://doi.org/10.12989/csm.2023.12.1.083.
21. Daouadji, T.H., Abbès, F., Bensatallah, T., Abbès, B. (2025). Analytical and numerical investigation of adhesive-bonded T-shaped steel–concrete composite beams for enhanced interfacial performance in civil engineering structures. Inventions, 10(4), 61. https://doi.org/10.3390/inventions10040061.
22. Benchohra, M., Laoufi, I., Attia, A., Bousahla, A.A., Tounsi, A., Tounsi, A., ... Mahmoud, S.R. (2025). Analytical solution for imperfect functionally graded beams resting on viscoelastic foundation. Structural Engineering and Mechanics, 95(2), 155-167. https://doi.org/10.12989/sem.2025.95.2.155.
23. Soares, P.B., Campos Filho, A., Lazzari, P.M., Lazzari, B.M., Pacheco, A.R. (2025). Finite element

analysis of reinforced concrete beams shear-strengthened with CFRP. Structural Engineering and Mechanics, 96(2), 155-166. https://doi.org/10.12989/sem.2025.96.2.155.

24. Tahar, H.D., Abderezak, R., Rabia, B. (2021). Hyperstatic steel structure strengthened with prestressed carbon/glass hybrid laminated plate. Coupled Systems Mechanics, 10(5), 393-414. https://doi.org/10.12989/csm.2021.10.5.393.
25. Aissa, B., Rabia, B., Tahar, H.D. (2023). Predicting and analysis of interfacial stress distribution in RC beams strengthened with composite sheet using artificial neural network. Structural Engineering and Mechanics, 87(6), 517-527. https://doi.org/10.12989/sem.2023.87.6.517.
26. Han, S.J., Kim, M.S., Heo, I., Lee, W.J., Lee, D. (2025). Performances of precast concrete composite double wall systems with discontinuous steel members as shear connector. Steel and Composite Structures, 55(4), 283. https://doi.org/10.12989/scs.2025.55.4.283.
27. Daouadji, T.H., Abderezak, R., Rabia, B. (2022). New technique for repairing circular steel beams by FRP plate. Advanced Materials Research, 11(3), 171-190. https://doi.org/10.12989/amr.2022.11.3.171.
28. Bouzid, H., Rabia, B., Daouadji, T.H. (2023). Ultimate behavior of RC beams strengthened in flexure using FRP material. Engineering Structures, 289, 116300. https://doi.org/10.1016/j.engstruct.2023.116300.
29. Habibi, A., Mollazadeh, M., Bazrafkan, A., Ademovic, N. (2023). Comparative analysis of multiple mathematical models for prediction of consistency and compressive strength of ultra-high performance concrete. Coupled Systems Mechanics, 12(6), 539-555. https://doi.org/10.12989/csm.2023.12.6.539.
30. Tahar, H.D., Boussad, A., Abderezak, R., Rabia, B., Fazilay, A., Belkacem, A. (2019). Flexural behaviour of steel beams reinforced by carbon fibre reinforced polymer: experimental and numerical study. Structural Engineering and Mechanics, 72(4), 409-419. https://doi.org/10.12989/sem.2019.72.4.409.
31. Abderezak, R., Daouadji, T.H., Rabia, B. (2022). Analysis and modeling of hyperstatic RC beam bonded by composite plate symmetrically loaded and supported. Steel and Composite Structures, 45(4), 591-603. https://doi.org/10.12989/scs.2022.45.4.591.
32. Seo, Y., Ju, H., Lee, D. (2025). Flexural strength of reinforced concrete members strengthened by fabric reinforced cementitious matrix considering bond characteristics. Structural Engineering and Mechanics, 94(2), 71-83. https://doi.org/10.12989/sem.2025.94.2.071.
33. Abderezak, R., Daouadji, T.H., Rabia, B. (2021). Modeling and analysis of the imperfect FGM-damaged RC hybrid beams. Advances in Computational Design, 6(2), 117-133. http://doi.org/10.12989/acd.2021.6.2.117.